

Abstract

We describe a new functionality within the Weather Research and Forecasting model with coupled Chemistry (WRF-Chem) that allows simulating emission, transport, dispersion, transformation and sedimentation of pollutants released during volcanic activities. Emissions from both an explosive eruption case and relatively calm degassing situation are considered using the most recent volcanic emission databases. A preprocessor tool provides emission fields and additional information needed to establish the initial three-dimensional cloud umbrella/vertical distribution within the transport model grid, as well as the timing and duration of an eruption. From this source condition, the transport, dispersion and sedimentation of the ash-cloud can be realistically simulated by WRF-Chem using its own dynamics, physical parameterization as well as data assimilation. Examples of model validation include a comparison of tephra fall deposits from the 1989 eruption of Mount Redoubt (Alaska), and the dispersion of ash from the 2010 Eyjafjallajökull eruption in Iceland. Both model applications show good coincidence between WRF-Chem and observations.

1 Introduction

Past and recent volcanic eruptions, such as Eyjafjallajökull (Gudmundsson et al., 2010) and Puyehue Cordon-Caulle (BGVM, 2011), with huge impacts on the environment (soil, water), air quality and air traffic have been increasing the need of accurate real time forecasts of ash movement and sedimentation and others hazardous products. Currently, most existing volcanic ash transport and dispersion (VATD) models involve a de-coupled or “offline” treatment of the physics and chemistry characterizing atmospheric-dispersion of volcanic emissions, and numerical weather prediction. See WMO (2010) for a report on the various available VATD models. However, interactions between the erupting plume and surrounding meteorological conditions could significantly affect the settling of volcanic ash/aerosol particles. As a consequence,

GMDD

5, 2571–2597, 2012

Inclusion of Ash and SO₂ emissions from volcanic eruptions in WRF-CHEM

M. Stuefer et al.

[Title Page](#)

[Abstract](#)

[Introduction](#)

[Conclusions](#)

[References](#)

[Tables](#)

[Figures](#)



[Back](#)

[Close](#)

[Full Screen / Esc](#)

[Printer-friendly Version](#)

[Interactive Discussion](#)



Inclusion of Ash and SO₂ emissions from volcanic eruptions in WRF-CHEM

M. Stuefer et al.

[Title Page](#)

[Abstract](#)

[Introduction](#)

[Conclusions](#)

[References](#)

[Tables](#)

[Figures](#)

[⏪](#)

[⏩](#)

[◀](#)

[▶](#)

[Back](#)

[Close](#)

[Full Screen / Esc](#)

[Printer-friendly Version](#)

[Interactive Discussion](#)



necessary parameters are the scale of the eruption including the erupted mass, the initial altitudes of the ash particles and SO₂, an eruption rate, and a grain size spectrum of the ash particles. Mastin et al. (2009) have developed “Eruption Source Parameters (ESP)” for the world’s volcanoes. Each of the world’s volcanoes has a “typical” eruption assigned to them. Mastin et al. (2009) provide details on each source parameter for each ESP type, which include plume altitude, mass of the eruption cloud and particle size distributions. WRF-Chem uses the ESP type data as volcanic emission information for the model forecasting. The volcanic ash model includes as source a number of 10 different bins representing the size spectrum of the particles typically ranging from a few micrometers up to one or two millimeters. We have developed a volcanic emission data generator package for system initialization using a look-up table containing the ESP data. The programming code of the Coupled Aerosol-Tracer Transport model, which has been developed for the Brazilian version of the Regional Atmospheric Modeling System (Freitas et al., 2009), has been used as template and adapted to suit WRF-Chem. In the following subsection we describe how ash and SO₂ emissions from volcanic activities are formulated for use in the WRF-Chem model.

2.1 The emissions preprocessor

To determine ash emission fields during volcanic eruption events, we use an emission-preprocessing tool (Freitas et al., 2011) following the database developed by Mastin et al. (2009). This database provides a set of parameters to model volcanic ash cloud transport and dispersion during eruptions. There is information on 1535 volcanoes around the world comprising location (latitude, longitude and height) as well as the corresponding historical parameters of plume height, mass eruption rate, volume rate, duration of eruption and the mass fraction of erupted debris finer than about 63 μm (see Table 1). Note that all parameters from this default database may be overwritten by the user once more accurate information is available. The emissions preprocessing tool provides the location of the volcano in the nearest model grid box and the emission parameters (i.e. mass eruption rate, plume height and time duration), if no other

Inclusion of Ash and SO₂ emissions from volcanic eruptions in WRF-CHEM

M. Stuefer et al.

[Title Page](#)

[Abstract](#)

[Introduction](#)

[Conclusions](#)

[References](#)

[Tables](#)

[Figures](#)

[⏪](#)

[⏩](#)

[◀](#)

[▶](#)

[Back](#)

[Close](#)

[Full Screen / Esc](#)

[Printer-friendly Version](#)

[Interactive Discussion](#)

observations are given. This information is used within WRF-Chem to determine the vertical distribution of the erupted mass. Large volcanic plumes are typically “umbrella” shaped (Sparks, 1997), i.e. their vertical distribution is shaped as detailed in Fig. 1. We use this observation – which may be modified by users – and assume that 75 % of the erupted mass is detrained in the umbrella cloud and 25 % beneath, with a linear distribution from the umbrella to the vent. The base of the umbrella cloud is roughly located at 73 % of the plume height. Figure 1 shows an example of the vertical profile of the ash-cloud mass distribution associated with an eruption with 12 km height above the vent, while the cloud base is located around 9 km height above it. Note the umbrella cloud detrainment layer is represented as a parabolic mass distribution with 75 % of the erupted mass. Twenty-five % of the erupted mass is linearly detrained from the umbrella base to the vent height. The total erupted mass is calculated using the correspondent erupted volume (Table 1) times the ash mass density, which is defined as 2600 kg m^{-3} . Then the total ash mass is distributed between 10 bins of aerosol particles with diameter size range starting from 2 mm down to less than $3.9 \mu\text{m}$, using the correspondent percentage of mass derived from analysis of historic eruptions. Table 2 gives the selected particle size bins, which have been associated with the WRF-Chem variable names vash_1 to vash_10, and the corresponding mass fraction percentage for each volcano ESP type. Scollo et al. (2007), Rose et al. (2007), Durant and Rose (2009), Bonadonna and Houghton (2005), Durant et al. (2009), and Bonadonna et al. (2002) used analysis of ash samples mostly from the example eruptions listed in Table 1 to derive the mass fraction percentage shown in Table 2. For each bin, the aerodynamic radius, needed by the settling velocity calculation, is defined as half of the arithmetic mean between the limits of the diameters of each bin size. The time interval during which the ash mass is released in the domain of the model simulation is given by the default “duration” parameter as specified in Table 1. If observed data of injection height h and eruption length d are available, they may be used instead. The 1535 volcanoes with referenced source parameters as specified in Table 1, for which WRF-Chem is able to simulate the associated ash-cloud movement in an event of eruption, are shown in

Fig. 2. This figure shows the geographical location in the world and also depicts the prescribed plume height above the vent.

2.2 Volcanic SO₂ degassing emissions

The data provided by the AEROCOM program (http://www-lscedods.cea.fr/aerocom/AEROCOM_HC/volc/, Diehl, 2009; Diehl et al., 2012) contains volcanic SO₂ emissions and other variables for all days from 1 January 1979 to 31 December 2009 for all volcanoes with historic eruptions listed in the Global Volcanism Program database provided by the Smithsonian Institution. There is one file for each year that contains the number of events for each day of that year over the entire world. For each event the volcano name, date, height above the mean sea level, cloud column height, longitude, latitude and daily emission rate of SO₂ are provided. There is also a separation between eruptive and non-eruptive volcanic emissions.

In similar fashion to the volcanic ash, the emissions processing tool places the SO₂ emissions from each volcano in the grid box, which surrounds its geographical location. The total emission is calculated by summing the emissions of all volcanoes within the grid cell. Next, the total emission and the minimum and maximum column heights of the set of volcanoes within the grid cell are provided. The units are kg [SO₂] m⁻² dy⁻¹. If other observed volcanic SO₂ emission data are available (i.e. from satellite retrievals using the Ozone Monitoring Instrument), or SO₂ emissions are modeled for volcanic eruptions outside the date range covered by the AEROCOM data, SO₂ mass emission rates can be entered in the WRF-Chem emissions driver. In this case the SO₂ plume resembles the umbrella shaped plume of the emitted ash as described above.

In general, once airborne, SO₂ oxidizes to sulfuric acid (H₂SO₄) that condenses into sulfate aerosol, and the atmospheric loading and residence time of the sulfate aerosol is proportional to the sulfur-containing gases in the volcanic plume. As for the ash emissions, -to evaluate the impacts of volcanic emissions, it is important to use accurate assumptions not only on SO₂ emission rates, but also on injection heights. It is important to note that SO₂ may show different plume characteristics than volcanic ash;

Inclusion of Ash and SO₂ emissions from volcanic eruptions in WRF-CHEM

M. Stuefer et al.

Title Page

Abstract

Introduction

Conclusions

References

Tables

Figures



Back

Close

Full Screen / Esc

Printer-friendly Version

Interactive Discussion



also the residence time of sulfate aerosol may differ significantly from the residence time of ash. An example was the June 1991 eruption of Pinatubo (Philippines), which injected large amounts of SO₂ and ash up to 35 km (a.s.l.) into the stratosphere. The sulfate aerosol was detected for many months after the eruption, while the ash settled within several days (McCormick et al., 1995).

3 Inclusion of volcanic emissions in WRF-Chem

In this section we describe how ash and SO₂ emissions from volcanic activities are used in the WRF-Chem model. WRF-Chem V3.4 contains two hard coded gas-phase chemical mechanisms (the second generation Regional Acid Deposition Model Mechanism (RADM2) (Stockwell et al., 1990), and the Carbon-Bond Mechanism version Z (CBM-Z) (Zaveri and Peters, 1999). The Kinetic PreProcessor (KPP, Salzmann, 2008, Grell et al., 2011) is also used in WRF-Chem, which allows many additional gas-phase chemical mechanisms. The three aerosol modules available in WRFV3.4 are the Modal Aerosol Dynamics Model for Europe (MADE) (Ackermann et al., 1998) with the secondary organic aerosol (SOA) model (SORGAM) of Schell et al. (2001) (referred to as MADE/SORGAM), and the Model for Simulating Aerosol Interactions and Chemistry (MOSAIC) (Zaveri et al., 2008). The Volatility Basis Set (VBS) approach has also been coupled to both, MOSAIC (Shrivastava et al., 2011) and MADE (Ahmadov et al., 2012). The numerically very simple and computationally inexpensive bulk approach from the Goddard Chemistry Aerosol Radiation and Transport (GOCART, Chin et al., 2002) model is also available in WRF-Chem V3.4. An aerosol optical property module (Fast et al., 2006, Barnard et al., 2010) was added to WRF-Chem that treats bulk, modal, and sectional aerosol size distribution using a similar methodology for refractive indices and multiple mixing rules. The interactions between aerosols and clouds, such as the first and second indirect effects, activation/resuspension, wet scavenging, and aqueous chemistry are described in more detail by Gustafson et al. (2007) and Chapman et al. (2009).

Inclusion of Ash and SO₂ emissions from volcanic eruptions in WRF-CHEM

M. Stuefer et al.

[Title Page](#)

[Abstract](#)

[Introduction](#)

[Conclusions](#)

[References](#)

[Tables](#)

[Figures](#)

[⏪](#)

[⏩](#)

[◀](#)

[▶](#)

[Back](#)

[Close](#)

[Full Screen / Esc](#)

[Printer-friendly Version](#)

[Interactive Discussion](#)



Inclusion of Ash and SO₂ emissions from volcanic eruptions in WRF-CHEM

M. Stuefer et al.

Title Page

Abstract

Introduction

Conclusions

References

Tables

Figures



Back

Close

Full Screen / Esc

Printer-friendly Version

Interactive Discussion

asymmetry parameter at 4 wavelengths (300, 400, 600 and 999 nm), with bin summation or extinction weighted averaging used to derive the integrated parameters. Wavelength interpolation based on Ångström coefficients for these 3 quantities is used as input for two radiative transfer options within WRF-Chem (the WRF Rapid Radiative Transfer Model (RRTMG, Iacono et al., 2008), or the Goddard shortwave scheme, Chou et al., 1998).

Additionally, SO₂ emissions are added to the gas-phase SO₂ variable, if SO₂ is available for the chosen chemistry option. Although these much more complex chemistry setups come with a heavy computational burden, more sophisticated studies of the impact of volcanic eruptions on air quality, weather, and short term climate can be undertaken.

While the emissions preprocessor provides not only volcano location, but also total mass and injection height, the latter will most often be overwritten by the user in the WRF-Chemnamelist, assuming that observations are available that are much closer to the truth. For historic cases with known injection heights h and duration d of an eruption, the default initialization parameters are then replaced by the total erupted mass m (kg), which is empirically derived from h (m) and d (s) according to Mastin et al. (2009):

$$m = \rho d (0.0005 h)^{4.1494} \quad (1)$$

The variable ρ denotes the assumed magma density of 2600 kg m⁻³. Figure 3 shows the mass eruption rate m/d in (kg s⁻¹) derived from Eq. (1), which increases significantly with injection height. It is evident that the total mass strongly depends on accurate injection heights. A 500 m error in d at an assumed injection height of 5 km amounts to a mass eruption rate error of about 40 tons per second; the same 500 m error increases to 1400 tons per second at an injection height of 15 km.

The model results of the impact of an eruption are obviously very sensitive to correct estimates of the plume characteristics. Data assimilation methods have been developed to improve the accuracy of the modeled state of the atmosphere and its

composition. It is important to note that WRF offers options to apply three and four dimensional data assimilation. In the case of volcanic emissions, satellite retrievals of characteristics of the ash and SO₂ (i.e. concentrations, aerosol optical depth, chemical composition) may be useful to correct for possible uncertainties in initial mass estimates or plume characteristics through data assimilation methods.

4 Some initial applications

All following experiments with WRF-Chem use versions 3.1 to 3.4 (Grell et al., 2005) that employs the Advanced Research WRF dynamical core (ARW, Skamarock et al., 2005) with the following parameterizations of physical processes: Mellor-Yamada-Janjić (MYJ) boundary layer parameterization (Janjić, 2002); Noah land-surface model (Chen and Dudhia, 2001); Grell-Devenyi convective parameterization (Grell and Devenyi, 2002); WRF Single-Moment-5 (WSM-5) microphysics (Hong et al., 2004); Goddard shortwave radiation scheme (Chou et al., 1998); Rapid Radiative Transfer Model longwave radiation (RRTM, Mlawer et al., 1997). For the results displayed below, no chemical interactions are taking place. In all simulations WRF-Chem is run with 10 volcanic ash species, including grid (advection and diffusion) and sub-grid transport processes (boundary layer vertical mixing, parameterized deep convection), as well as dry deposition, wet deposition, and settling of ash.

4.1 The prediction of ash fall

To show the capability of the model to predict ash-fall, we chose to simulate the 1989 Redoubt eruption in Alaska; see Casadevall (1994) and Miller and Chouet (1994) for more information on the eruption. Some observations of tephra fall deposits were available to us for this period (see Scott and McGimsey, 1994). Although this was also an interesting case for transport of volcanic ash – a KLM B747 briefly lost all of its engines when flying through the ash cloud (Casadevall, 1994) – upper air observational data

Inclusion of Ash and SO₂ emissions from volcanic eruptions in WRF-CHEM

M. Stuefer et al.

[Title Page](#)

[Abstract](#)

[Introduction](#)

[Conclusions](#)

[References](#)

[Tables](#)

[Figures](#)

[⏪](#)

[⏩](#)

[◀](#)

[▶](#)

[Back](#)

[Close](#)

[Full Screen / Esc](#)

[Printer-friendly Version](#)

[Interactive Discussion](#)



were not available. To show the transport properties of the modeling system, we therefore decided to use the Eyjafjallajökull volcano in another application presented in the next subsection.

For Redoubt 1989, we focus on the first 2 major explosive eruptions that together only lasted for 23 min and occurred on 14 December 1989, 19:00 UTC. Miller and Chouet (1994) reported an injection height of more than 10 km above sea level for the 2 eruption events, thus we used an assumed injection height of 12 km for the WRF-Chem initialization. WRF-Chem, with its setup described above, was started at 14 December 1989, 00:00 UTC, and run for a 48 h period. Figure 4 compares results of the total ash-fall predictions with observations of tephra deposited from 14 to 15 December 1989. The WRF-Chem model was able to capture the pattern of the ash-fall as measured in the tephra deposits. The volcanic ash in WRF-Chem was injected at an altitude where winds were predictable over the short time periods that we are studying. However, there was a close resemblance in the magnitudes of the predicted tephra fall deposits with the observed data. One also has to take into account the large uncertainty of the total mass injected as well as the uncertainty of the assumed size distribution (Carey and Sigurdsson, 1982).

4.2 Simulation of ash transport for Eyjafjallajökull

Next we show results from WRF-Chem runs of the Eyjafjallajökull Volcano in Iceland, April of 2010. A detailed evaluation of this case is presented in Webley et al. (2012). WRF-Chem was initialized with volcanic plume altitudes derived from the local weather radar station (IMO, 2010), a S2 ESP type particle size distribution (compare Table 2), and a source mass according to Eq. (1). Continuous model simulations including a series of explosive eruptions were performed from 14 April, 00:00 UTC for 5 days until 19 April, 00:00 UTC. Figure 5 shows the Eyjafjallajökull ash cloud dispersing initially towards the east and southeast extending over Central Europa on the 15 April. The ash dispersed further over Europe and to the east towards northern Russia during the following days, and shifting winds over the North Atlantic from the 18 to 19 April 2010

Inclusion of Ash and SO₂ emissions from volcanic eruptions in WRF-CHEM

M. Stuefer et al.

[Title Page](#)

[Abstract](#)

[Introduction](#)

[Conclusions](#)

[References](#)

[Tables](#)

[Figures](#)



[Back](#)

[Close](#)

[Full Screen / Esc](#)

[Printer-friendly Version](#)

[Interactive Discussion](#)



dispersed ash to the West, south of Greenland. WRF-Chem resulted in ash concentrations over Central Europe between $0.5\text{--}2\text{ mg m}^{-3}$ at altitudes between 4 and 6 km (Webley et al., 2012). We compared the modeled concentrations with satellite volcanic ash retrievals and LIDAR measurements at several measurement locations in Europe (Webley et al., 2012). For Leipzig, the LIDAR showed an ash layer around 4 km a.s.l. passing over the region from 13:47–15:32 UTC on 16 April 2010 (Fig. 6a). WRF-Chem showed an ash cloud pass over Leipzig between 10:00 and 15:00 UTC. The cloud was around 5 km a.s.l. as it first passed over the site and closer 3 km a.s.l. by the end (Fig. 6b). Ash concentrations at around 11:00 UTC reached $800\text{ }\mu\text{g m}^{-3}$ ($0.8\text{ }\mu\text{g m}^{-3}$). A vertical profile to coincide with the LIDAR data (Fig. 6c) showed an ash layer from 2–4 km a.s.l. with a peak the concentration at 3.5 km a.s.l. Ansmann et al. (2010) showed from post-processed LIDAR data that the cloud was centered at 3.5 km and had ash concentrations around $900\text{ }\mu\text{g m}^{-3}$. The WRF-Chem modeled magnitude proved to be close to the LIDAR data.

5 The software

The software tool necessary to produce the input data to WRF-Chem simulates the movement of volcanic ash-cloud and/or SO_2 is the PREP-CHEM-SRC emission tool (Freitas et al., 2011). This system is coded using Fortran90 and C and requires Hierarchical Data Format (HDF) and Network Common Data Format (NetCDF) libraries. The desired grid configuration and emission inventories to provide emission fluxes and additional information are defined in a Fortran *namelist* file called “prep-chem-src.inp”. The software has been tested with GFortran, Intel and Portland Fortran compilers under the UNIX/LINUX operating system. Emissions output from the PREP-CHEM-SRC program are provided in separate intermediate binary data files for volcanic emissions as well as anthropogenic emissions, biomass burning, GOCART aerosol background fields if so desired.

Inclusion of Ash and SO_2 emissions from volcanic eruptions in WRF-CHEM

M. Stuefer et al.

[Title Page](#)

[Abstract](#)

[Introduction](#)

[Conclusions](#)

[References](#)

[Tables](#)

[Figures](#)

[⏪](#)

[⏩](#)

[◀](#)

[▶](#)

[Back](#)

[Close](#)

[Full Screen / Esc](#)

[Printer-friendly Version](#)

[Interactive Discussion](#)

A utility program, `convert_emiss`, is provided with the WRF-Chem model that converts these separate intermediate files from PREP-CHEM-SRC into WRF input data files. This utility program reads the volcanic emissions binary data file, computes the vertical mass distribution and the emissions for the volcanic ash size bin before populating the emissions input data arrays. The WRF-Chem model then reads the input data and then either re-computes the emissions based upon a new eruption height and vertical mass distribution provided as a WRF-Chem input parameter, or uses the prescribed volcanic ash emissions.

6 Summary and conclusions

A volcanic eruption plume model was added successfully to WRF-Chem. Several options are available in WRF-Chem to treat the transport and fall out of volcanic ash. Initial implementations include options to study the long-range dispersion of small ash particles smaller than $63\ \mu\text{m}$ using only 2 to 4 ash-bin variables. In order to model ash deposition as well as atmospheric transport of ash, subsequently 10 ash variables were added to WRF-Chem describing the typical bin size distribution of the total ash during a volcanic eruption event.

The total ash is distributed into the model bins according to a typical particle distribution scheme, which is characteristic for each eruption type. During an eruption event, the ash is distributed in an umbrella-shape vertical distribution plume above the volcano. Eruption source parameters have been compiled from historic eruptions (Mastin et al., 2009); the source parameters are characteristic for certain eruption types, and have been assigned to 1535 volcanoes worldwide. The parameters were implemented as a look-up table in the WRF-ChemPREP-CHEM-SRC emission tool. The data include injection heights and the duration of an event, and represent the best initial assessment of the type and size of future eruptions. In addition to ash, volcanic SO_2 sources were added from the AEROCOM program. Alternatively to the AEROCOM dataset, SO_2 was implemented in WRF-Chem by distributing the ash in an umbrella shaped

Inclusion of Ash and SO_2 emissions from volcanic eruptions in WRF-CHEM

M. Stuefer et al.

[Title Page](#)

[Abstract](#)

[Introduction](#)

[Conclusions](#)

[References](#)

[Tables](#)

[Figures](#)

[⏪](#)

[⏩](#)

[◀](#)

[▶](#)

[Back](#)

[Close](#)

[Full Screen / Esc](#)

[Printer-friendly Version](#)

[Interactive Discussion](#)



plume in similar fashion to the ash. The SO₂ initial mass is also estimated as a first guess.

This implementation offers opportunities for the operational community to use this tool for prediction of hazardous events. Additionally scientists may try to improve their understanding of the interaction of volcanic aerosols with radiation and microphysics.

Studies with different volcanic ash source models are in progress to test the sensitivity of the various eruption source parameters. Obviously the initial ash particle size distribution and the associated mass are critical for the downwind ash concentrations. So far there are no aggregation effects included in the model, since there are no aggregation observational data and only very vague model theories in existence.

Acknowledgements. The authors acknowledge support from the US Air Force Weather Agency and the University of Alaska Arctic Region Supercomputing Center. This publication results in part of research sponsored by the Cooperative Institute for Alaska Research with funds from the National Oceanic and Atmospheric Administration under cooperative agreement NA08OAR4320751 with the University of Alaska. S. R. Freitas acknowledges partial support of this work by CNPq (302696/2008-3).

References

- Ackermann, I. J., Hass, H., Memmesheimer, M., Ebel, A., Binkowski, F. S., and Shankar, U.: Modal aerosol dynamics model for Europe: Development and first applications, *Atmos. Environ.*, 32, 2981–2999, 1998.
- Ahmadov, R., McKeen, S. A., Robinson, A., Bahreini, R., Middlebrook, A., de Gouw, J., Meagher, J., Hsie, E., Edgerton, E., Shaw, S., and Trainer, M.: A volatility basis set model for summertime secondary organic aerosols over the eastern United States in 2006, *J. Geophys. Res.*, 117, D06301, doi:10.1029/2011JD016831, 2012.
- Ansmann, A., Tesche, M., Groß, S., Freudenthaler, V., Seifert, P., Hiebsch, A., Schmidt, J., Wandinger, U., Mattis, I., Müller, D., and Wiegner, M.: The 16 April 2010 major volcanic ash plume over central Europe: EARLINET lidar and AERONET photometer observations at Leipzig and Munich, Germany, *Geophys. Res. Lett.*, 37, L13810, doi:10.1029/2010GL043809, 2010.

GMDD

5, 2571–2597, 2012

Inclusion of Ash and SO₂ emissions from volcanic eruptions in WRF-CHEM

M. Stuefer et al.

Title Page

Abstract

Introduction

Conclusions

References

Tables

Figures



Back

Close

Full Screen / Esc

Printer-friendly Version

Interactive Discussion



Inclusion of Ash and SO₂ emissions from volcanic eruptions in WRF-CHEM

M. Stuefer et al.

[Title Page](#)

[Abstract](#)

[Introduction](#)

[Conclusions](#)

[References](#)

[Tables](#)

[Figures](#)



[Back](#)

[Close](#)

[Full Screen / Esc](#)

[Printer-friendly Version](#)

[Interactive Discussion](#)



Barnard, J. C., Fast, J. D., Paredes-Miranda, G., Arnott, W. P., and Laskin, A.: Technical Note: Evaluation of the WRF-Chem “Aerosol Chemical to Aerosol Optical Properties” Module using data from the MILAGRO campaign, *Atmos. Chem. Phys.*, 10, 7325–7340, doi:10.5194/acp-10-7325-2010, 2010.

5 Bonadonna, C. and Houghton, B. F.: Total grain-size distribution and volume of tephrafall deposits, *Bull. Volc.* 67, 441–456, 2005.

Bonadonna, C., Mayberry, G. C., Calder, E. S., Sparks, R. S. J., Choux, C., Jackson, A. M., Lejeune, A. M., Loughlin, S. C., Norton, G. E., Rose, W. I., Ryan, G., and Young, S. R.: Tephra fallout in the eruption of Soufrière Hills Volcano, Montserrat, in: *The eruption of Soufrière Hills Volcano, Montserrat, from 1995 to 1999*, edited by: Druitt, T. H. and Kokelaar, B. P. Geological Society of London, London, 483–516, 2002.

10 Bulletin of the Global Volcanism Network: BGVN, Weekly report of Puyehue-CordónCaulle volcano, 1 June–7 June 2011, available at: <http://www.volcano.si.edu/world/volcano.cfm?vnum=1507-15> (last access: 9 July 2012), 2011.

15 Carey, S. N. and Sigurdsson, H.: Influence of particle aggregation on deposition of distal tephra from the May 18, 1980, eruption of Mount St. Helens volcano, *J. Geophys. Res.*, 87, 7061–7072, 1982.

Casadevall, T. J.: The 1989/1990 eruption of Redoubt Volcano Alaska: impacts on aircraft operations, *J. Volcanol. Geoth. Res.*, 62, 301–316, 1994.

20 Chapman, E. G., Gustafson Jr., W. I., Easter, R. C., Barnard, J. C., Ghan, S. J., Pekour, M. S., and Fast, J. D.: Coupling aerosol-cloud-radiative processes in the WRF-Chem model: Investigating the radiative impact of elevated point sources, *Atmos. Chem. Phys.*, 9, 945–964, doi:10.5194/acp-9-945-2009, 2009.

25 Chen, F. and Dudhia, J.: Coupling an advanced land-surface/hydrology model with the Penn State/NCAR MM5 modeling system, Part I: Model description and implementation, *Mon. Weather Rev.*, 129, 569–585, 2001.

Chin, M., Ginoux, P., Kinne, S., Holben, B. N., Duncan, B. N., Martin, R. V., Logan, J., Higurashi, A., and Nakajima, T.: Tropospheric aerosol optical thickness from the GOCART model and comparisons with satellite and sunphotometer measurements, *J. Atmos. Sci.*, 59, 461–483, 2002.

30 Chou, M. D., Suarez, M. J., Ho, C. H., Yan, M. M. H., and Lee, K. T.: Parameterizations for cloud overlapping and shortwave single-scattering properties for use in general circulation and cloud ensemble models, *J. Climate*, 11, 202–214, 1998.

Inclusion of Ash and SO₂ emissions from volcanic eruptions in WRF-CHEM

M. Stuefer et al.

[Title Page](#)[Abstract](#)[Introduction](#)[Conclusions](#)[References](#)[Tables](#)[Figures](#)[⏪](#)[⏩](#)[◀](#)[▶](#)[Back](#)[Close](#)[Full Screen / Esc](#)[Printer-friendly Version](#)[Interactive Discussion](#)

- Diehl, T.: A global inventory of volcanic SO₂ emissions for hindcast scenarios, available at: <http://www-lscedods.cea.fr/aerocom/AEROCOMHC/> (last access: 16 April 2010), 2009.
- Diehl, T., Heil, A., Chin, M., Pan, X., Streets, D., Schultz, M., and Kinne, S.: Anthropogenic, biomass burning, and volcanic emissions of black carbon, organic carbon, and SO₂ from 1980 to 2010 for hindcast model experiments, *Atmos. Chem. Phys. Discuss.*, submitted, 2012.
- Durant, A. J. and Rose, W. I.: Sedimentological constraints on hydrometeor-enhanced particle deposition: 1992 Eruptions of Crater Peak, Alaska, *J. Volcanol. Geoth. Res.*, 186, 40–59, doi:10.1016/j.jvolgeores.2009.02.004, 2009.
- Durant, A. J., Rose, W. I., Sarna-Wojcicki, A. M., Carey, S., and Volentik, A. C.: Hydrometeor-enhanced tephra sedimentation: Constraints from the 18 May 1980 eruption of Mount St. Helens (USA), *J. Geophys. Res.*, 114, B03204, doi:10.1029/2008JB005756, 2009.
- Fast, J. D., Gustafson Jr., W. I., Easter, R. C., Zaveri, R. A., Barnard, J. C., Chapman, E. G., Grell, G. A., and Peckham, S. E.: Evolution of ozone, particulates, and aerosol direct radiative forcing in the vicinity of Houston using a fully coupled meteorology-chemistry-aerosol model, *J. Geophys. Res.*, 111, D21305, doi:10.1029/2005JD006721, 2006.
- Freitas, S. R., Longo, K. M., Silva Dias, M. A. F., Chatfield, R., Silva Dias, P., Artaxo, P., Andreae, M. O., Grell, G., Rodrigues, L. F., Fazenda, A., and Panetta, J.: The Coupled Aerosol and Tracer Transport model to the Brazilian developments on the Regional Atmospheric Modeling System (CATT-BRAMS) – Part 1: Model description and evaluation, *Atmos. Chem. Phys.*, 9, 2843–2861, doi:10.5194/acp-9-2843-2009, 2009.
- Freitas, S. R., Longo, K. M., Alonso, M. F., Pirre, M., Marecal, V., Grell, G., Stockler, R., Mello, R. F., and Sánchez Gácita, M.: PREP-CHEM-SRC – 1.0: a preprocessor of trace gas and aerosol emission fields for regional and global atmospheric chemistry models, *Geosci. Model Dev.*, 4, 419–433, doi:10.5194/gmd-4-419-2011, 2011.
- Grell, G. A. and Baklanov, A.: Integrated Modeling for Forecasting Weather and Air Quality: A Call for Fully Coupled Approaches, *Atmos. Environ.*, 45, 6845–6851, doi:10.1016/j.atmosenv.2011.01.017, 2011.
- Grell, G. A. and Devenyi, D.: A generalized approach to parameterizing convection combining ensemble and data assimilation techniques, *Geophys. Res. Lett.*, 29, 1693, doi:10.1029/2002GL015311, 2002.
- Grell, G. A., Peckham, S. E., Schmitz, R., McKeen, S. A., Frost, G., Skamarock, W. C., and Eder, B.: Fully coupled “online” chemistry within the WRF model, *Atmos. Environ.*, 39, 6957–6975, 2005.

Inclusion of Ash and SO₂ emissions from volcanic eruptions in WRF-CHEM

M. Stuefer et al.

[Title Page](#)
[Abstract](#)
[Introduction](#)
[Conclusions](#)
[References](#)
[Tables](#)
[Figures](#)
[Back](#)
[Close](#)
[Full Screen / Esc](#)
[Printer-friendly Version](#)
[Interactive Discussion](#)

Grell, G. A., Fast, J., Gustafson, W. I., Peckham, S. E., McKeen, S. A., Salzmann, M., and Freitas, S.: On-Line Chemistry within WRF: Description and Evaluation of a State-of-the-Art Multiscale Air Quality and Weather Prediction Model, in: *Integrated Systems of Meso-Meteorological and Chemical Transport Models*, edited by: Baklanov, A., Mahura, A., and Sokhi, R., Springer, 2011.

Gudmundsson, M. T., Pedersen, R., Vogfjörð, K., Thorbjarnardóttir, B., Jakobsdóttir, S., and Roberts, M. J.: Eruptions of Eyjafjallajökull Volcano, Iceland. *Eos*, 91, 190–191, 2010.

Gustafson Jr., W. I., Chapman, E. G., Ghan, S. J., Easter, R. C., and Fast, J. D.: Impact on Modeled Cloud Characteristics Due to Simplified Treatment of Uniform Cloud Condensation Nuclei During NEAQS 2004, *Geophys. Res. Lett.*, 34, L19809, doi:10.1029/2007GL030021, 2007.

Hong, S. Y., Dudhia, J., and Chen, S. H.: A revised approach to ice-microphysical processes for the bulk parameterization of cloud and precipitation, *Mon. Weather Rev.*, 132, 103–120, 2004.

Iacono, M. J., Delamere, J. S., Mlawer, E. J., Shephard, M. W., Clough, S. A., and Collins, W. D.: Radiative forcing by long-lived greenhouse gases: Calculations with the AER radiative transfer models, *J. Geophys. Res.*, 113, D13103, doi:10.1029/2008JD009944, 2008.

Icelandic Meteorological Office (IMO): Eyjafjallajökull 2010 plume altitude measured by weather radar, available at: <http://andvari.vedur.is/~arason/radar/> (last access: May 2011), 2010.

Janjić, Z. I.: Nonsingular implantation of the Mellor–Yamada level 2.5 scheme in the NCEP mesomodel, NOAA/NWS/NCEP Office Note 437, 61 pp., 2002.

Mastin, L., Guffanti, M., Servranckx, R., Webley, P., Barsotti, S., Dean, K., Durant, A., Ewert, J., Neri, A., and Rose, W.: A multidisciplinary effort to assign realistic source parameters to models of volcanic ash-cloud transport and dispersion during eruptions, *J. Volcanol. Geoth. Res.*, 186, 10–21, 2009.

McCormick, M. P., Thomason, L. W., and Trepte, C. R.: Atmospheric effects of the Mt. Pinatubo eruption, *Nature*, 373, 399–404, doi:10.1038/373399a0, 1995.

Miller, T. P. and Chouet, B. A.: The 1989–1990 eruptions of Redoubt volcano: an introduction, in: *The 1989–1990 eruptions of Redoubt Volcano, Alaska*, edited by: Miller, T. P. and Chouet, B. A., *J. Volcanol. Geoth. Res.*, 62, 1–10, 1994.

Mlawer, E. J., Taubman, S. J., Brown, P. D., Iacono, M. J., and Clough, S. A.: Radiative transfer for inhomogeneous atmosphere: RRTM, a validated correlated-k model for the longwave, *J. Geophys. Res.*, 102, 16663–16682, 1997.

Inclusion of Ash and SO₂ emissions from volcanic eruptions in WRF-CHEM

M. Stuefer et al.

[Title Page](#)

[Abstract](#)

[Introduction](#)

[Conclusions](#)

[References](#)

[Tables](#)

[Figures](#)

[⏪](#)

[⏩](#)

[◀](#)

[▶](#)

[Back](#)

[Close](#)

[Full Screen / Esc](#)

[Printer-friendly Version](#)

[Interactive Discussion](#)

- Pruppacher, H. R. and Klett, J. D.: Microphysics of Clouds and Precipitation, 2nd Edn., Kluwer Academic Publishers, Dordrecht, The Netherlands, 954 pp., 1997.
- Rose, W. I., Kostinski, A. B., and Kelley, L.: Real time C band radar observations of 1992 eruption clouds from Crater Peak/Spurr Volcano, Alaska, U.S.G.S. Bulletin 2139, Spurr Eruption, edited by: Keith, T., 19–26, 1995.
- Rose, W. I., Self, S., Murrow, P. J., Ernst, G. J., Bonadonna C., and Durant, A. J.: Pyroclastic fall deposit from the October 14, 1974 eruption of Fuego Volcano, Guatemala, Bull. Volc., 70, 1043–1067, doi:10.1007/s00445-007-0187-5, 2007.
- Salzmann, M.: WRF-Chem/KPP Coupler (WKC) for WRF V3, Users' and Developers Guide v2.0, Princeton University, Princeton, NJ, 2008.
- Schell, B., Ackermann, I. J., Hass, H., Binkowski, F. S., and Ebel, A.: Modeling the formation of secondary organic aerosol within a comprehensive air quality modeling system, J. Geophys. Res., 106, 28275–28293, 2001.
- Scollo, S., Del Carlo, P., and Coltelli, M.: Tephra fallout of 2001 Etna rank eruption: Analysis of the deposit and plume dispersion, J. Volcanol. Geoth. Res., 160, 147–164, 2007.
- Scott, W. E. and McGimsey, R. G.: Character, mass, distribution, and origin of tephra-fall deposits of the 1989–1990 eruption of Redoubt Volcano, south-central Alaska, in: The 1989–1990 Eruptions of Redoubt Volcano, Alaska, edited by: Miller, T. P. and Chouet, B. A., J. Volcanol. Geotherm. Res., 62, 251–272, 1994.
- Shrivastava, M., Fast, J., Easter, R., Gustafson Jr., W. I., Zaveri, R. A., Jimenez, J. L., Saide, P., and Hodzic, A.: Modeling organic aerosols in a megacity: comparison of simple and complex representations of the volatility basis set approach, Atmos. Chem. Phys., 11, 6639–6662, doi:10.5194/acp-11-6639-2011, 2011.
- Skamarock, W. C., Klemp J. B., Dudhia, J., Gill, D. O., Barker, D. M., Wang, W., and Powers, J. G.: A description of the advanced research WRF version 2, NCAR Technical Note, NCAR/TN-468+STR, 88 pp., 2005.
- Sparks, R. S. J., Bursik, M. I., Carey, S. N., Gilbert, J. S., Glaze, L. S., Sigurdsson, H., and Woods, A. W.: Volcanic Plumes, John Wiley and Sons, Sussex, 574 pp., 1997.
- Stockwell, W. R., Middleton, P., Chang, J. S., and Tang, X.: The second generation regional acid deposition model chemical mechanism for regional air quality modeling, J. Geophys. Res., 95, 16343–16367, 1990.

Inclusion of Ash and SO₂ emissions from volcanic eruptions in WRF-CHEM

M. Stuefer et al.

Title Page

Abstract

Introduction

Conclusions

References

Tables

Figures

⏪

⏩

◀

▶

Back

Close

Full Screen / Esc

Printer-friendly Version

Interactive Discussion

Webley, P. W. and Mastin, L. G.: Improved Prediction and tracking of Volcanic Ash clouds, J. Volcanol. Geoth. Res., Special Issue on Volcanic Ash Clouds, edited by: Mastin, L. and Webley, P., 186, 1–9, doi:10.1016/j.jvolgeores.2008.10.022, 2009.

5 Webley, P. W., Steensen, T., Stuefer, M., Grell, G. A., Freitas, S., and Pavolonis, M.: Analyzing the Eyjafjallajokull 2010 eruption using satellite remote sensing, lidar and WRF-Chem dispersion and tracking model, J. Geophys. Res., 117, D00U26, doi:10.1029/2011JD016817, 2012.

10 World Meteorological Organization (WMO): Workshop on Ash Dispersal forecast and civil aviation: model definition document, available at: <http://www.unige.ch/sciences/terre/mineral/CERG/Workshop/results/Model-Document-Geneva10.pdf> (last access: 16 April 2011), 2010.

Zaveri, R. A. and Peters, L. R.: A new lumped structure photochemical mechanism for large-scale applications, J. Geophys. Res., 104, 30387–30415, 1999.

15 Zaveri, R. A., Easter, R. C., Fast, J. D., and Peters, L. K.: Model for simulating aerosol interactions and chemistry, J. Geophys. Res., 113, D13204, doi:10.1029/2007JD008782, 2008.

Inclusion of Ash and SO₂ emissions from volcanic eruptions in WRF-CHEM

M. Stuefer et al.

Table 1. Injection height, duration, eruption rate, volume and mass fraction (< 63 μm) as provided by Mastin et al. (2009) and used to determine the eruption properties within the WRF-Chem model. Adapted from Mastin et al. (2009).

ESP	Type	Example	Height above vent (km)	Duration (h)	Eruption rate (kg s ⁻¹)	Volume (km ³)	Mass fraction less than 63 micron
M0	Standard mafic	Cerro Negro. Nicaragua. 13 Apr 1992	7	60	1.00 × 10 ⁵	0.01	0.05
M1	small mafic	Etna. Italy. 19–24 Jul 2001	2	100	5.00 × 10 ³	0.001	0.02
M2	medium mafic	Cerro Negro. Nicaragua. 9–13 Apr 1992	7	60	1.00 × 10 ⁵	0.01	0.05
M3	large mafic	Fuego. Guatemala. 14 Oct 1974	10	5	1.00 × 10 ⁶	0.17	0.1
S0	standard silicic	Spurr. USA. 18 Aug 1992	11	3	4.00 × 10 ⁶	0.015	0.4
S1	small silicic	Ruapehu. New Zealand. 17 Jun 1996	5	12	2.00 × 10 ⁵	0.003	0.1
S2	medium silicic	Spurr. USA. 18 Aug 1992	11	3	4.00 × 10 ⁶	0.015	0.4
S3	large silicic	St. Helens. USA. 18 May 1980	15	8	1.00 × 10 ⁷	0.15	0.5
S8	co-ignimbrite silicic	St. Helens. USA. 18 May 1980 (pre-9 AM)	25	0.5	1.00 × 10 ⁸	0.05	0.5
S9	Brief silicic	Soufrière Hills. Montserrat (composite)	10	0.01	3.00 × 10 ⁶	0.0003	0.6
U0	default submarine	none	0	–	–	–	–

[Title Page](#)
[Abstract](#)
[Introduction](#)
[Conclusions](#)
[References](#)
[Tables](#)
[Figures](#)
[Back](#)
[Close](#)
[Full Screen / Esc](#)
[Printer-friendly Version](#)
[Interactive Discussion](#)

Inclusion of Ash and SO₂ emissions from volcanic eruptions in WRF-CHEM

M. Stuefer et al.

Table 2. Ash particle bin size ranges with corresponding WRF-Chem variable names; the mass fractions in percent of total mass are given below each ESP eruption type M0–M3 and S0–S9.

Particle Size Bin	Phi	WRF Var	M0	M1	M2	M3	S0	S1	S2	S3	S8	S9
1–2 mm	–1–0	vash_1	6.5	0.0	6.5	13.0	22.0	24.0	22.0	2.9	2.9	0.0
0.5–1 mm	0–1	vash_2	12.0	4.0	12.0	20.0	5.0	25.0	5.0	3.6	3.6	0.0
0.25–0.5 mm	1–2	vash_3	18.8	10.0	18.8	27.5	4.0	20.0	4.0	11.8	11.8	0.0
125–250 μm	2–3	vash_4	36.3	50.0	36.3	22.5	5.0	12.0	5.0	8.2	8.2	9.0
62.5–125 μm	3–4	vash_5	20.5	34.0	20.5	7.0	24.5	9.0	24.5	7.9	7.9	22.0
31.25–62.5 μm	4–5	vash_6	3.0	2.0	3.0	4.0	12.0	4.3	12.0	13.0	13.0	23.0
15.625–31.25 μm	5–6	vash_7	1.5	0.0	1.5	3.0	11.0	3.3	11.0	16.3	16.3	21.0
7.8125–15.625 μm	6–7	vash_8	1.0	0.0	1.0	2.0	8.0	1.3	8.0	15.0	15.0	18.0
3.9065–7.8125 μm	7–8	vash_9	0.5	0.0	0.5	1.0	5.0	0.8	5.0	10.0	10.0	7.0
<3.9 μm	> 8	vash_10	0.0	0.0	0.0	0.0	3.5	0.5	3.5	11.2	11.2	0.0

Title Page

Abstract

Introduction

Conclusions

References

Tables

Figures

⏪

⏩

◀

▶

Back

Close

Full Screen / Esc

Printer-friendly Version

Interactive Discussion

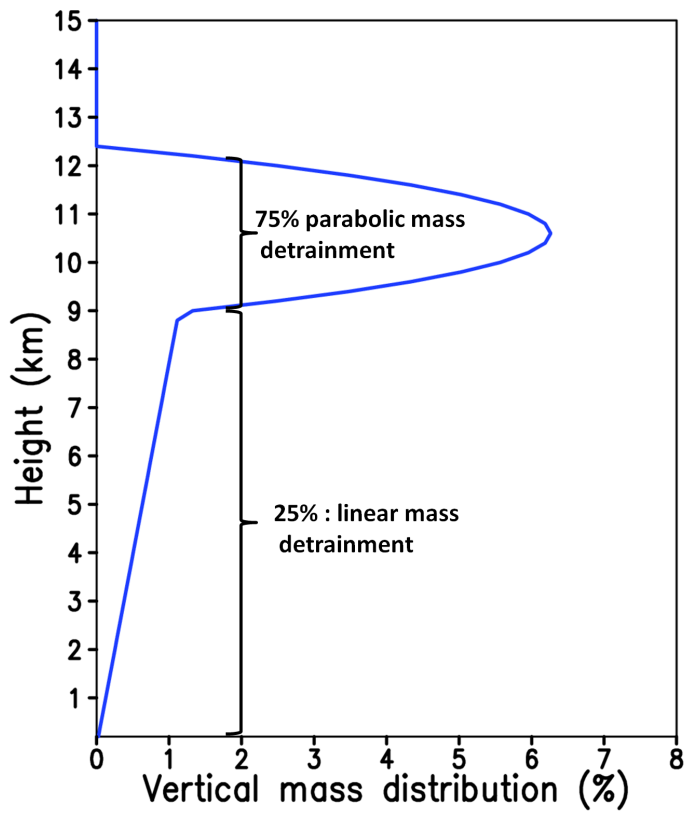


Fig. 1. The vertical profile of the ash-cloud mass distribution (%) associated with an eruption with 12 km height above the vent. In this case, the cloud base is located around 9 km height above the vent. Note the umbrella cloud detrainment layer represented as a parabolic mass distribution with 75 % of the erupted mass. The 25 % of the erupted mass is linearly detrained from the umbrella base to the vent height.

Inclusion of Ash and SO₂ emissions from volcanic eruptions in WRF-CHEM

M. Stuefer et al.

[Title Page](#)

[Abstract](#) [Introduction](#)

[Conclusions](#) [References](#)

[Tables](#) [Figures](#)

[◀](#) [▶](#)

[◀](#) [▶](#)

[Back](#) [Close](#)

[Full Screen / Esc](#)

[Printer-friendly Version](#)

[Interactive Discussion](#)



**Inclusion of Ash and
SO₂ emissions from
volcanic eruptions in
WRF-CHEM**

M. Stuefer et al.

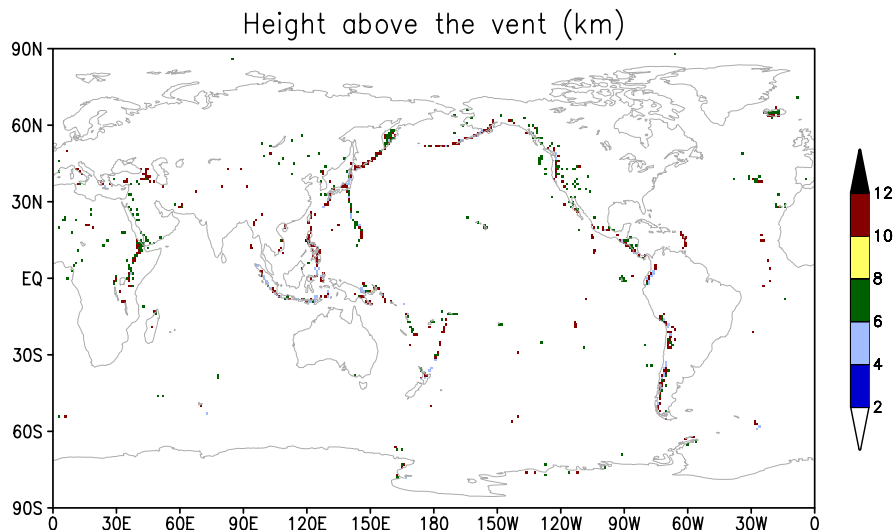


Fig. 2. The global dataset of volcanoes described in Mastin et al. (2009) and included in WRF-Chem model do simulate ash-cloud movement. The figure shows the plume height above the vent prescribed for each volcano with past and potential future eruption.

[Title Page](#)[Abstract](#)[Introduction](#)[Conclusions](#)[References](#)[Tables](#)[Figures](#)[⏪](#)[⏩](#)[◀](#)[▶](#)[Back](#)[Close](#)[Full Screen / Esc](#)[Printer-friendly Version](#)[Interactive Discussion](#)

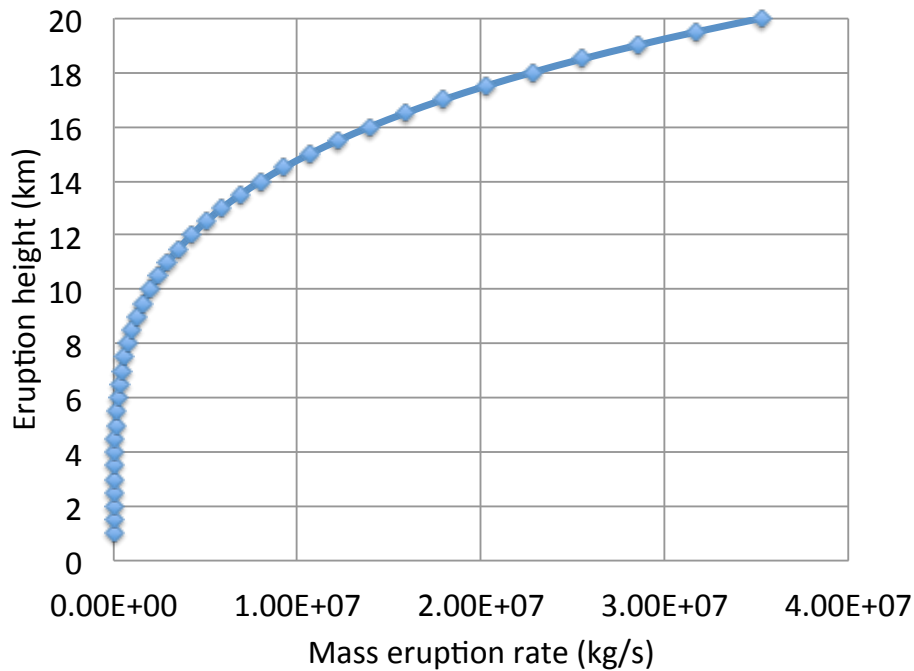


Fig. 3. Mean mass eruption rates derived from injection heights.

Inclusion of Ash and SO₂ emissions from volcanic eruptions in WRF-CHEM

M. Stuefer et al.

Title Page

Abstract	Introduction
Conclusions	References
Tables	Figures

⏪	⏩
◀	▶
Back	Close

Full Screen / Esc

Printer-friendly Version

Interactive Discussion



Inclusion of Ash and SO₂ emissions from volcanic eruptions in WRF-CHEM

M. Stuefer et al.

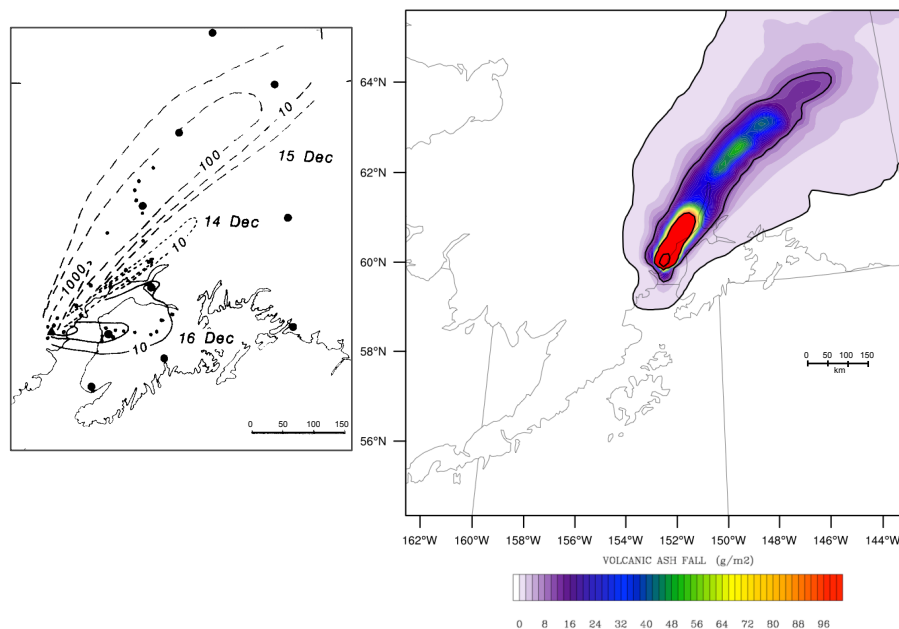


Fig. 4. Measured tephra-fall deposits (g m^{-2}) and derived isopachs (left, adapted from Scott and McGimsey, 1994) and WRF-Chem modeled ash-fall (right) of the 1989 eruption of Redoubt Volcano, south-central Alaska.

[Title Page](#)[Abstract](#)[Introduction](#)[Conclusions](#)[References](#)[Tables](#)[Figures](#)[⏪](#)[⏩](#)[◀](#)[▶](#)[Back](#)[Close](#)[Full Screen / Esc](#)[Printer-friendly Version](#)[Interactive Discussion](#)

Inclusion of Ash and SO₂ emissions from volcanic eruptions in WRF-CHEM

M. Stuefer et al.

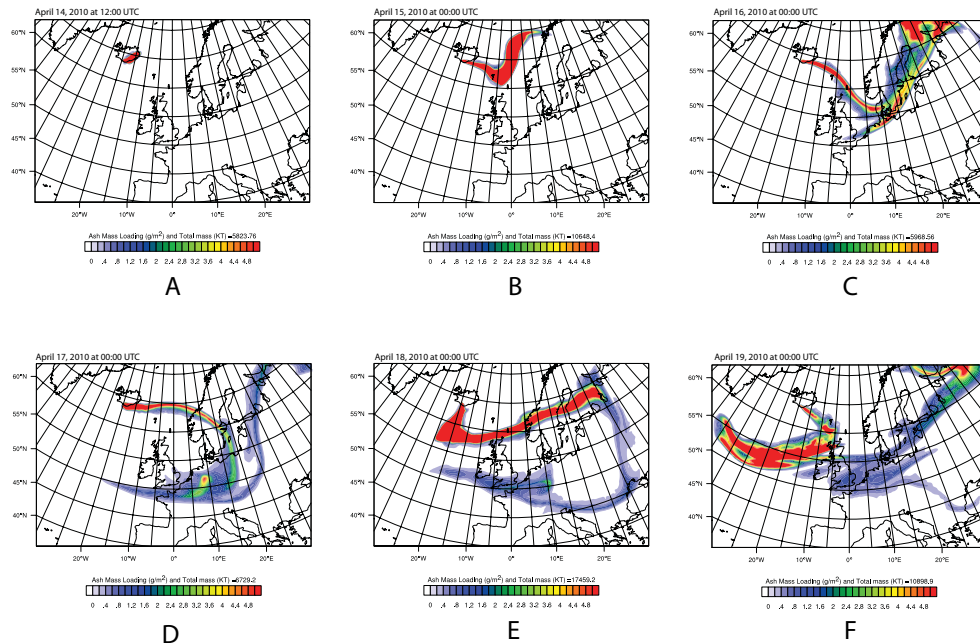


Fig. 5. Daily WRF-Chem dispersion of the Eyjafjallajökull ash mass loading from 14 April 2010 (A) to the 19 April 2010 (F). Adapted from Webley et al. (2012).

Title Page

Abstract

Introduction

Conclusions

References

Tables

Figures



Back

Close

Full Screen / Esc

Printer-friendly Version

Interactive Discussion

Inclusion of Ash and SO₂ emissions from volcanic eruptions in WRF-CHEM

M. Stuefer et al.

Title Page

Abstract

Introduction

Conclusions

References

Tables

Figures

◀

▶

◀

▶

Back

Close

Full Screen / Esc

Printer-friendly Version

Interactive Discussion

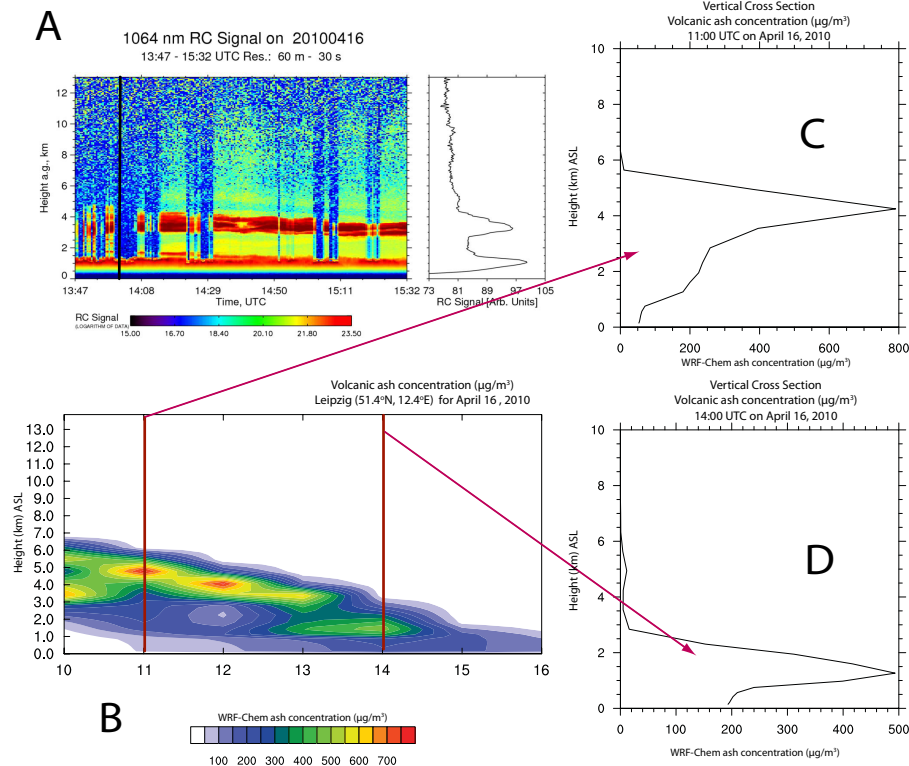


Fig. 6. (A) Earlinet LIDAR at Leipzig, Germany on 16 April from 13:47–15:32 UTC, (B) WRF-Chem simulation from 10:00–16:00 UTC and (C, D) vertical profiles at 11:00 and 14:00 UTC, respectively (adapted from Webley et al., 2012).